NASA CR 130251

ANALYSIS OF FLIGHT TEST

TRANSITION AND TURBULENT HEATING DATA

(NASA-CR-130251) ANALYSIS OF FLIGHT TEST TRANSITION AND TURBULENT HEATING DATA. PART 2: TURBULENT HEATING RESULTS Final Report, Jun. A.L. Laganelli (General Electric Co.) Nov. 1972 20 p CSCL 20D G3/12 N73-12288 Unclas 48277

PART II - TURBULENT HEATING RESULTS

A. L. Laganelli

GENERAL ELECTRIC COMPANY
PHILADELPHIA, PA.

FOREWORD

The present report is one of a series of two which define the post flight evaluation of a series of ballistic flight test boundary layer transition and turbulent heating data. Part I presents the resultsof the boundary layer transition investigation (NASA CR 129045). Part II presents the results of the turbulent heating investigation.

These reports document the work performed under Contract No. NASW-2234, for the period June 1971 through October 1972. The investigation was conducted for National Aeronautics and Space Administration Headquarters Division with Mr. Alfred Gessow as the NASA technical monitor.

The authors wish to express their appreciation to the following General Electric Company personnel: Dr. F Alyea, Mr. A. Birnbaum, Mr. T. Harper, Dr. C. Kyriss, and Ms. E. Storer.

TABLE OF CONTENTS

Section		Page
	FOREWORD	
	NOMENCLATURE	
1	INTRODUCTION	1
2	ASSESSMENT OF PREVIOUS WORK	4
3	PRESENT STUDY	5
4	DATA REDUCTION	6
5	RESULTS	7
6	CONCLUSIONS	11
7	REFERENCES	12
Apprndix		
A	TRANSFORMATION FUNCTIONS	14

NOMENCLATURE

A	constant
B	constant
C_f, C_F	skin friction coefficient — local and average
F_C, F_X, F_θ	transformation functions
h, H	static and total enthalpy
k	Configuration factor (zero for flat plate, unity for axisymmetric bodies)
M_e	boundary layer edge Mach number
n	exponent in viscosity law
Pr	Prandtl number
R_N, R_B	nose and base radius
Re	Reynolds number
r	recovery factor or radial coordinate (axisymmetric body)
St	Stanton number
T	absolute temperature
u, v	velocity components in the x and y directions
x, y	coordinates, parallel and normal to the stream
α	angle of attack also hyperbolic angle
β	hyperbolic angle
γ	ratio of specific heats
ϵ_T	turbulent compressibility factor,
θ_c	cone half angle
μ	absolute viscosity
ρ	density
τ	shear stress

Subscripts

e	boundary layer edge
w	wall
i	incompressible
x	based on length (axial)
s	based on wetted length (equal to x for flat plate)
θ	based on momentum thickness
aw	adiabatic wall

Superscripts

0	total
*	based on reference temperature

SECTION 1

INTRODUCTION

The problem associated with the effect of nonisothermal and compressible conditions, relative to the laws of heat transfer and skin friction, in turbulent boundary layers has received considerable attention in the scientific community. In general, theories have been developed that predict the frictional drag coefficient in the compressible turbulent boundary layer and modified forms of the Reynolds analogy have been invoked to determine the heat transfer characteristics. Moreover, the variations in the assumptions used by the authors allow for a general classification of the theories, namely; (a) analysis employing the von Karman or Prandtl differential equations, (b) analysis exercising other differential equations, (c) analysis based upon a fixed velocity profile, (d) analysis based upon the incompressible formulation with fluid properties evaluated at a reference state, and (e) semi-empirical analysis based upon experimental data.

Spalding and Chi[1], who employed the latter technique above, reviewed and summarized the governing equations and assumptions used in the more popular concepts. The wide divergence of the various theories is quite dramatically illustrated in Figure 1 (which was obtained from the works of Chapman and Kester[2]). As a consequence of these discrepancies, Spalding and Chi compared a large number of data (heat transfer and skin friction) for supersonic flow with nineteen (19) different theories. The best results, based on a total R.M.S. error, from their study were the theories of van Driest II[3], Kutateladze and Leont'ev[4], Wilson[5], and Spalding and Chi[1].

Examination of re nt literature indicates that the works of van Driest II, Spalding and Chi, and the reference state type[6, 7] received a considerable amount of attention. These techniques have been shown to provide good agreement with ground test data and, in principle, are easy to use. This latter condition is desirable, inasmuch as it makes their use very attractive to the design engineer. Basically, van Driest employs the von Karman mixing length concept and Crocco temperature distribution with the Prandtl shear-stress equation. On the other hand, Spalding and Chi developed a semi-empirical technique that did not allow for a choice of mixing length or viscosity power law. However, a function for transforming the skin friction coefficient was assumed to be the same as that used by van Driest. The transformation functions were derived from experimental skin friction data that was limited to low Mach numbers (supersonic range). Finally, the reference state techniques, as in Spalding-Chi, did not employ a mixing length concept but assumed a transformation of C_f and R_{e_θ} to an incompressible plane. The thermodynamic properties contained in the above parameters were evaluated at some reference enthalpy (or temperature) that is a function of M_e, T_w, and T_{aw}. Such an approach for arbitrary shape bodies was developed by Walker[8] and was used herein.

Since the wide variation in the semi-empirical concepts require data for validation, recourse to experiments is necessary. Essentially, the compressible turbulent boundary layer heat transfer or skin friction behavior, relative to the prediction techniques, has been shown to be a function of the Mach number, Reynolds number, and ratio of wall to boundary layer edge (or total) temperature, such that:

$$St = f\left[M_e, Re, T_w/T_e\right]$$

$$C_f = g\left[M_e, Re, T_w/T_e\right]$$

where the heat transfer or skin friction coefficient is usually expressed as a function of one of the variables with the remaining two as parameters.

One now has the choice of transforming the incompressible theories to a compressible plane in which case comparisons can be made to the compressible boundary layer data, or the compressible data can be transformed to an incompressible plane using a particular transforming technique (such as van Driest, Spalding-Chi, etc). In the latter condition, comparisons can be made to an acceptable incompressible skin friction relationship, such as Karman-Schoenherr, which has been shown to be valid over a wide range of Reynolds number.

A brief review of several recent and pertinent documents consists of the work of Bertram and Neal[9] who examined several experiments in hypersonic turbulent boundary layers with the intent of comparing these results with flight data. The authors were concerned with the effect of Mach number and wall temperature on the heat transfer and found that both flight data and ground test data did not consistently support any one theory.

Hopkins et al[10] measured local skin friction and heat transfer on flat plates, cones, and a wind tunnel wall for a range of Mach number and wall to adiabatic wall temperature ratio. Data were compared to the theories of References (1), (3), (7), and (11) where it was found that the heat transfer predictions for non-adiabatic conditions favored the works of van Driest II and Coles, provided the correct Reynolds analogy factor was employed. This work was subsequently followed by another investigation[12] to determine local skin friction behavior on a flat plate. These results were used to evaluate eight (8) theories on a generalized basis by transforming the data onto an incompressible skin friction curve. The results indicate than the van Driest II and Coles theories, when based on a momentum thickness Reynolds number, give the best prediction.

Cary[13] critically reviewed the Reynolds analogy between turbulent heat transfer and skin friction from data of several experiments and concluded that these data cannot, in general, be used to validate methods of predicting turbulent skin friction until a comprehensive definition of the Reynolds analogy is available. Finally,

Zoby and Graves[14] examined the prediction techniques of van Driest II, Spalding and Chi, and Eckert (reference state) using turbulent heating data from wind tunnels as well as free-flight tests. The authors found that the Spalding-Chi and Schultz-Grunow[15] (which employs the Eckert reference enthalpy) methods using the Colburn analogy give the best agreement with the Reynolds number based on distance from the peak heating point in the former and on distance from the transition location for the latter. Moreover, the best agreement with only the wind tunnel data was obtained with the Spalding-Chi technique using the von Karman form of the Reynolds analogy and Reynolds number based on distance from peak heating. On the other hand, the reference enthalpy technique using the Colburn analogy gave the best agreement to the free flight data for a Reynolds number based on distance from the transition location.

SECTION 2

ASSESSMENT OF PREVIOUS WORK

An examination of experimental data[9], [10], [12], [14] obtained for various geometric configurations, Mach number ranges, and ratio of wall temperature to adiabatic wall temperature variations, indicate that the aforementioned prediction techniques are adequate for the adiabatic wall condition of Mach numbers up to 4. However, at hypersonic Mach number conditions, a variation in the prediction techniques existed for both adiabatic and non-adiabatic wall conditions, particularly $T_w/T_{aw} < 0.3$ which is indicative of flight conditions.

In assessing the various turbulent heating prediction techniques, it appears that the work of van Driest II, Spalding-Chi, and the reference state (Eckert) have received the most attention. However, as noted above, other techniques were examined. A brief review of the aforementioned techniques as well as other methods is given in Reference (12). It should be noted that the Russian work of Kutateladze and Leont'ev[4] appears to have been neglected in the literature.

Some of the pertinent conclusions resulting from the above studies include:

(1) The van Driest II, Spalding-Chi, and reference state (Eckert) methods predict heat transfer with reasonable success when the proper form of the Reynolds analogy was used.

(2) Use of momentum thickness Reynolds number in the skin friction relations avoided use of an arbitrary virtual origin.

(3) Employing the techniques of (1) together with a Reynolds number based on distance (from peak heating or transition onset) appears to correlate both wind tunnel and flight data on the incompressible plane. However it should be noted that a knowledge of this distance (peak heating or transition) is difficult to determine a priori.

(4) Calculations appear to correlate both flat plate and axisymmetric bodies when the Mangler factor is used.

(5) For an adiabatic wall condition, a comparison of the theories appears reasonable for $M<4$. However, for $M>4$, Spalding and Chi method has a tendency to underpredict the data

(6) For a non-adiabatic flat plate ($T_w/T_{aw} > 0.3$), the theory of van Driest gives a reasonable prediction of skin friction. At lower temperature ratios there is still some question concerning the best method; however, the reference techniques appears to be the most favorable.

SECTION 3

PRESENT STUDY

In general, skin friction (momentum equation) results have been a basis for the various prediction techniques and recourse to modified forms of the Reynolds analogy are used to determine heat transfer results. The integral form of the momentum equation has been commonly used as a consequence of its ease of computation. This investigation was concerned with comparing the three aforementioned concepts with flight data. In particular, several flight vehicles were investigated that contain sufficient on-board instrumentation such that a detailed evaluation of the measured data could be assessed relative to the functions required to transform the compressible data onto an incompressible plane. The flight cases consisted of slender non-ablating shields (Beryllium) with ATJ graphite noses. Moreover, attention was focused on altitudes after transition (turbulent heating) where angle-of-attack effects were minimized (e.g., $\alpha / \theta_c \lesssim 0.1$).

As a result of the ablative nose materials used on flight vehicles, the effect of nose bluntness and the subsequent shape change on local properties along the frustum were considered. Figures 2 and 3 show the local edge Mach number and wetted length Reynolds number at the aft end of a six degree half angle cone as a function of bluntness ratio for both a spherically blunted nose and a typical laminar ablated shape. These results were computed using the GE Viscous Interaction Zero Angle-of-Attack Drag[16] (VIZAAD) program. During re-entry, the nose of the vehicle recedes creating an aerodynamic shape change which, in turn, affects the flow field characteristics. The amount of stagnation point recession depends upon the nose material where the local properties typically vary from the solid line (spherical) to the dashed line shown in Figures 2 and 3. The significance of this effect varies, depending upon the trajectory flown, the nose material, and the initial bluntness of the vehicle. It is observed for that vehicles with bluntness ratios of $R_N/R_B \rightarrow 0.04$ to 0.20 in. that the nose shape has a marked effect and should be accounted for in the determination of local properties.

Accordingly, this investigation considered the shape change of the ablated nose during re-entry which, in turn, was used as an input to an inviscid flow field[17] calculation that provided the pressure distribution and shock shape. This result was then used in the VIZAAD program to determine the local properties in the boundary layer at a prescribed point in the trajectory. The transformation functions for the various theories were then determined to reduce the compressible data to the incompressible plane. The transformation functions that relate the compressible and incompressible planes have been documented[12], [14], [18] and are restated within as Appendix A.

SECTION 4

DATA REDUCTION

Inasmuch as the techniques studied in this investigation required transformation functions to convert compressible data onto an incompressible plane, a standard format for the incompressible plane was established. The Karman-Schoenherr skin friction relation has been an accepted standard since it was shown to agree with incompressible data over a wide range of Reynolds number. Figures 4 and 5 show the skin friction coefficient as a function of Reynolds number, based on distance and momentum thickness respectively, for several theories. It is noted that the explicit relation of Walker is an excellent agreement with the implicit relation of van Driest. Moreover, it is observed that the very simple explicit relations of Walker are in excellent agreement with the Karman-Schoenherr results.

The solid and dashed lines shown in Figures 6 and 7 represent the incompressible modified forms of the Reynolds analogy as a function of Reynolds number based on distance and momentum thickness, respectively. The curves were generated using a Prandtl number of 0.72 and the explicit skin friction relation of Walker. Inasmuch as the skin friction relation of Walker is essentially the same as the Karman-Schoenherr result, these curves were used as the incompressible standard for the flight data comparisons.

The data search yielded 16 vehicles that had transition criteria that met the following requirements; (1) small angle-of-attack at transition onset ($\alpha / \theta_c \lesssim 0.1$), (2) post flight trajectory reconstruction, (3) simple sphere-cone geometry, (4) on-board sensors, and (5) non-ablating shields. From this list, seven vehicles were chosen for the data reduction and comparison to the turbulent heating theories. The choice of the seven was a consequence of the availability of inverse heat conduction solutions to obtain the net heat flux to the surface from the sensors or by some other calorimeter data reduction technique. In all cases, the thermal sensor at the most aft station was selected for the analysis (i.e., furthest from the end of transition).

The evaluation of the local properties at the sensor station required a definition of the free stream conditions as well as the ablated shape of the vehicle at the various altitudes during the trajectory. The RESEP[19] program was used to determine the shape of the ablative nosetip throughout re-entry. The shape change was used as an input condition to the flow field[17] program that considers a numerical solution of the inviscid shock layer for axisymmetirc bodies to provide shock shape and surface pressure distributions around the ablated shape. This, in turn, was used as an input to the VIZAAD[16] program that determines local boundary layer edge properties for axisymmetric bodies.

The following schematic represents the methodology used in reducing the flight data to the incompressible plane as well as determining the local properties in the flow field and subsequent transformation functions.

Given

Trajectory
Geometry → RESEP[19] → Shape Change @ Altitude of Interest
Material

↓

Input Into → FLOW FIELD[17] → Shock Shape/Pressure Distributions

↓

Input Into → VIZAAD[16] → Local properties
(also h_w) ρ, u, T, P, Re_θ, Re_x, $\dot{q}_w$, c_f, h, h_{aw}

↓

Determine Transformation Functions F_θ, F_X, F_C according to particular theory

↓

Given

Flight Data Sensor (T_w) and $\dot{q}_w$ (as obtained by an inverse heat conduction solution)

↓

Calculate Stanton Number: $St = \dot{q}_w/(\rho\, u)_e \; (h_{aw} - h_w)$

↓

Convert Compressible Data Onto The Incompressible Plane By Use of The Transformation Functions

$$St_i = F_C \, St$$

$$Re_{\theta_i} = F_\theta \, Re_\theta$$

$$Re_{x_i} = F_X \, Re_x$$

↓

Compare With Modified Forms of The Reynolds Analogy

Colburn

$$St_i = Pr^{-2/3} \frac{C_{f_i}}{2}$$

von Karman

$$St_i = \frac{C_{f_i}}{2}\left[1 + 5\sqrt{\frac{C_{f_i}}{2}}\left(Pr - 1 + \ln\left[\frac{5Pr+1}{6}\right]\right)\right]^{-1}$$

where (using Walkers Relations)

$$C_{f_i} = 0.01958\ (Re_{x_i})^{-0.131}$$

$$C_{f_i} = 0.01\ [Re_{\theta_i} - 1161]^{-0.1508}$$

Inasmuch as Re_θ is not a readily obtainable parameter in flight experiements, values of the Reynolds number based on wetted length were favored for the comparison basis. The local properties were obtained from the VIZAAD code using the input conditions shown on the schematic. Moreover, a Reynolds number based on wetted length emanating from the vehicle stagnation point was required as a consequence of the unreliability of selecting a virtual origin based on transition behavior.

As noted in Reference 12, use of the Reynolds number based on momentum thickness as a correlating parameter is less arbitrary then the assumptions required for a virtual origin. Moreover, theories that transform compressible skin friction (or heat transfer) data onto an incompressible Re_{θ_i} plane should also suffice for a Reynolds number based on distance (Re_{x_i}). Consequently, a method of determining the momentum thickness was required in order to use Re_{θ_i} as a correlating parameter. In this study, the procedure adapted by Walker[8] was used where modifications were made[18] to extend the range of Reynolds number. Essentially, Walker considered a particular solution to the combined momentum and energy equation that used a multiplicative factor to represent departures from the flat plate relations. An explicit relationship was determined for the heat transfer and skin friction relations. However, the above relations were found to be applicable in the Reynolds number range 10^5 to 10^7 when compared to experimental data. The procedure was modified[18] to account for Reynolds numbers greater than 10^7 using the Schultz-Grunow relations. The expression representing the compressible momentum thickness was given by

$$\theta = \frac{0.0371 \left\{ \int_0^x \rho_e u_e^{(2.25+1.25H)} \mu_e^{.25} (\epsilon_T r^k)^{1.25} dx \right\}^{4/5}}{\rho_e u_e^{(2+H)} r^k}$$

where:

H = Shape factor δ^*/θ

r = Radial coordinate (measured from axis of symmetry)

k = Configuration factor (zero for flat plate, unity for axisymmetric bodies)

ϵ_T = Turbulent compressibility factor $(\rho^*/\rho_e)^{4/5} (\mu^*/\mu_e)^{1/5}$

SECTION 5

RESULTS

Having established the local conditions at the sensor location, the transformation functions for each turbulent heating technique was evaluated. Table I lists the pertinent local properties and the transformation functions for the vehicles considered in this study. It is noted that each vehicle was examined at one or more altitudes. Also to be noted is that the heat transfer coefficient (Stanton number) is given by the equivalent flat plate value. This was accomplished by dividing the flight value by the Mangler factor (1.176 for turbulent boundary layer flow on a sharp cone).

The appropriate transformation function was used to reduce the compressible data onto an incompressible plane. The results of these transformations are shown in Figures 6 and 7. In the former, the incompressible Stanton number is shown as a function of Reynolds number based on wetted length. The three turbulent heating techniques are shown with the Colburn and von Karman forms of the Reynolds analogy. It appears that the reference enthalpy method best fits the flight data when the Colburn analogy is used, whereas the van Driest II method appears to be equally favorable fitting the data with both forms of the Reynolds analogy. On the other hand, the Spalding-Chi method underpredicts both forms of the modified Reynolds analogy.

Figure 7 shows the incompressible Stanton number as a function of the Reynolds number based on momentum thickness. Again, the reference enthalpy technique best fits the data when the Colburn analogy is used and the van Driest II method appears to fit the data equally well for both forms of the Reynolds analogy while the Spalding-Chi method is underpredicted.

5.1 FURTHER COMMENTS

In Figures 6 and 7, no attempt was made to consider a virtual origin effect, e.g., when the turbulent boundary layer initiates at some position on the cone other than the tip (see References 9 and 14). One reason for selecting the wetted length characteristics was that ablation effects from the nosetip tend to destablize the boundary layer. Moreover, insufficient data made the problem of selecting transition onset and peak heating locations at various altitudes almost impossible.

While the methodology in determining the local boundary layer edge properties was considered quite accurate, the techniques used in determining the net heat transfer to the surface of the various re-entry vehicles was questionable (for example, the type of inverse heat transfer code). This problem was compounded by the type of thermal sensors, installation techniques, and interpretation of raw data output information. It is believed that the major discrepancies in the evaluation of the flight data is a consequence of the errors which are implicit in the reported heat flux data obtained from the various documents. As a result, the Re-Entry F[14] data was used as a guideline to confirm the data reduction process inasmuch as the NASA-Langley vehicle is well documented and has received excellent evaluation.

SECTION 6

CONCLUSIONS

The results of the three turbulent heating predictions (van Driest II, Spalding-Chi), and Eckert) were compared to the data of several re-entry vehicles. The data analyzed covered a range of Mach number of 3.3 to 15.2, wall to boundary layer edge temperature ratio of .46 to 2.6, and Reynolds number of 7×10^6 to 5.3×10^8. Data were transformed to an incompressible plane, using existing prediction methods, and compared with the Colburn and von Karman modified forms of the Reynolds analogy.

The results indicate that the Eckert reference enthalpy technique best fits the data when the Colburn analogy is used; whereas, the van Driest II method appears to be in agreement with the data with both forms of the modified Reynolds analogy. The Spalding-Chi method tends to underpredict the data. Finally, there does not appear to be any significant difference when comparing the incompressible Stanton number as a function of Reynolds number based on either wetted length or momentum thickness.

SECTION 7

REFERENCES

1. Spalding, D.B. and Chi, S.W., "The Drag of a Compressible Turbulent Boundary Layer on a Smooth Flat Plate with and Without Heat Transfer", J. Fluid Mech., Vol. 18, Pt. 1, January, 1964, pp. 117-143.

2. Chapman, D.R. and Kester, R.H., "Measurements of Turbulent Skin Friction on Cylinders in Axial Flow at Subsonic and Supersonic Velocities", J.A.S., Vol. 20, No. 7, July 1963, p. 441.

3. Van Driest, E.F., "The Problem of Aerodynamic Heating", Aeron. Eng. Rev., Vol. 15; No. 10, October 1956, p. 26.

4. Kutateladze, S.S. and Leont'ev, A.I., Turbulent Boundary Layer in Compressible Gases, Academic Press, Inc., New York, 1964. (Also, Advances in Heat Transfer, Vol. 3, Academic Press, New York, 1966.)

5. Wilson, R.E., "Turbulent Boundary Layer Characteristics at Supersonic Speeds - Theory and Experiment", J. of Aero. Sci., Vol. 17, Sept. 1950, p. 585.

6. Eckert, E.R.G., "Engineering Relations for Heat Transfer and Friction in High Velocity Laminar and Turbulent Boundary Layer Flow Over Surfaces with Constant Pressure and Temperature", Trans. ASME, Vol. 78, No. 6, August 1956, p. 1273.

7. Sommer, S.C. and Short, B.J., "Free-Flight Measurements of Turbulent Boundary Layer Skin Friction in the Presence of Severe Aerodynamic Heating at Mach Numbers from 2.8 to 7.0", NASA TN-3391, 1955.

8. Walker, G.K., "A Particular Solution to the Turbulent Boundary Layer Equations", J. Aero. Sci., Vol. 27, No. 9, September 1960, p. 715. (Also GE AETM No. 156.)

9. Bertram, M.H. and Neal, L., "Recent Experiments in Hypersonic Turbulent Boundary Layers," NASA TMX-56335, May 1965.

10. Hopkins, E.J., Rubesin, M.W., Inouye, M., Keener, E.R., Mateer, G.C., and Polek, T.E., "Summary and Correlation of Skin-Friction and Heat-Transfer Data for a Hypersonic Turbulent Boundary Layer on Simple Shapes", NASA TN-D-5089, June 1969.

11. Coles, D., "The Turbulent Boundary Layer in a Compressible Fluid", Phys, Fluids, Vol. 7, No. 9, Sept. 1964.

12. Hopkins, E.J., Keener, E.R., and Louie, P.T., "Direct Measurements of Turbulent Skin Friction on a Non-Adiabatic Flat Plate at Mach Number 6.5 and Comparisons with Eight Theories", NASA TN D-5675, February 1970.

13. Cary, A.M., "Summary of Available Information on Reynolds Analogy for Zero-Pressure Gradient; Compressible, Turbulent Boundary Layer Flow", NASA TN-D-5560, January 1970.

14. Zoby, E.V. and Graves, R.H., "Comparison of Results from Three Prediction Methods with Turbulent Heating Data from Wind-Tunnel and Free-Flight Tests", NASA-TMX-2390, Sept. 1971.

15. Zoby, E.V. and Sullivan, E.M., "Correlation of Free-Flight Turbulent Heat-Transfer Data From Axisymmetric Bodies with Compressible Flat Plate Relationships", NASA TN D-3802, 1967.

16. Studerus, C.H. and Dienna, E.A., "Viscous Interaction Zero Angle of Attack Drag (VIZAAD)", TIS 64SD292, General Electric Company, November 1964.

17. Gravalos, F.G., Edelfelt, I.H., and Emmons, H.W., "The Supersonic Flow About a Blunt Body of Revolution for Gases at Chemical Equilibrium", Proc. of the 9th Annual Cong. Int. Astro. Fed., Amsterdam, 1958.

18. Laganelli, A.L., "Evaluation of Turbulent Heating Predictions with Flight Data", GE-TIS 72SD229, June 1972.

19. Chin, J.H., "Two Dimensional Thermochemical and Thermostructural Response of Graphite NoseTips" - Hardening Technology Study - Vol. III, Lockheed Missile/Space Division N-16-69-4, also SAMSO TR-69-181, March 1969.

APPENDIX A. TRANSFORMATION FUNCTIONS

FUNCTION	van DRIEST II[3]	SPALDING-CHI[1]	WALKER[8] (ECKERT REF. ENTHALPY)
$F_c = \frac{C_{f_i}}{C_f}$	$\frac{r\frac{\gamma-1}{2}M_e^2}{[\sin^{-1}\alpha + \sin^{-1}\beta]^2}$	Same as van Driest II	$\frac{\rho_e}{\rho^*}$
$F_\theta = \frac{Re_{\theta_i}}{Re_\theta}$	$\frac{\mu_e}{\mu_w} = \left(\frac{T_w}{T_e}\right)^{-n}$	$\left(\frac{T_w}{T_e}\right)^{-0.0702}\left(\frac{T_{aw}}{T_w}\right)^{0.722}$	$\frac{\mu_e}{\mu^*}$
$F_x = \frac{Re_{x_i}}{Re_x}$	$\frac{F_\theta}{F_c}$	$\frac{F_\theta}{F_c}$	$\frac{\rho^*\mu_e}{\rho_e\mu^*}$
	$\alpha = (2A^2 - B)/(B^2+4A^2)^{1/2}$ $\beta = B/(B^2+4A^2)^{1/2}$ $A^2 = \frac{r\frac{\gamma-1}{2}M_e^2}{T_w/T_e}$ $B = \frac{1+r\frac{\gamma-1}{2}M_e^2}{T_w/T_e} - 1$		ρ^* and μ^* evaluated at reference temperature T^* $T^*/T_e = \frac{1}{2} + \frac{1}{2}(T_w/T_e) + 0.11\, r\,(\gamma-1)\,M_e^2$ $n = \frac{3}{2} + \frac{\ell n\left(\frac{T_e+198.6}{T_w+198.6}\right)}{\ell n\left(\frac{T_w}{T_e}\right)}$

TABLE I. TRANSFORMATION FUNCTIONS AND PERTINENT LOCAL PROPERTIES

VEHICLE	M_e	Re_s	Re_θ	$\frac{T_w}{T_e}$	ECKERT			VAN DRIEST			SPALDING-CHI			n	St_{FP}
					F_c	F_θ	F_x	F_c	F_θ	F_x	F_c	F_θ	F_x		
B09	3.34	2.87^7	1.76^4	2.62	2.23	0.571	0.256	2.1	0.51	0.243	2.1	0.562	0.281	0.7	7.87^{-4}
B09	3.75	4.67^7	2.95^4	1.6	1.82	0.641	0.352	1.68	0.704	0.418	1.68	1.328	0.83	0.74	6.38^{-4}
B06	14.64	9.57^7	1.8^4	1.33	9.19	0.237	0.026	6.42	0.832	0.13	6.42	11.11	1.85	0.65	$1.62^{-4}/2.24^{-4}$
B13	4.06	7.1^6	9.95^3	0.46	1.34	0.843	0.628	1.17	1.58	1.35	1.17	8.94	7.98	0.58	1.28^{-3}
B01	15.14	1.51^8	2.93^4	1.34	9.77	0.205	0.021	6.57	0.813	0.124	6.57	11.52	1 845	0.695	1.7^{-4}
B01	15.18	3.42^8	5.4^4	1.8	10.02	0.223	0.022	7.51	0.68	0.096	7.1	7.49	1.12	0.65	1.49^{-4}
B01	15.2	5.28^8	7.55^4	2.1	10.23	0.221	0.022	7.22	0.62	0.086	7.22	6.04	0.89	0.65	1.41^{-4}
B05	11.58	5.0^7	1.76^4	0.57	5.79	0.320	0.055	3.84	1.44	0.375	3.84	26.7	6.95	0.65	$4.55^{-4}/2.28^{-4}$
B07	13.83	2.27^8	3.62^4	2.32	8.82	0.259	0.0294	6.21	0.59	0.095	6.21	4.46	0.718	0.62	1.82^{-4}
B08	7.77	4.23^7	1.52^4	0.67	3.08	0.503	0.163	2.29	1.28	0.56	2.29	8.87	3.87	0.61	6.03^{-4}
B13	3.43	2.63^7	2.3^4	1.22	1.55	0.762	0.492	1.43	0.884	0.617	1.43	1.77	1.24	0.62	5.41^{-4}
B06	14.3	1.48^8	2.62^4	1.98	9.16	0.242	0.026	7.0	0.646	0.0924	7.0	6.01	0.86	0.64	$1.73^{-4}/2.26^{-4}$
B07	14.15	1.64^8	2.89^4	1.81	8.91	0.246	0.028	6.13	0.684	0.112	6.13	10.16	1.66	0.64	1.81^{-4}
B05	11.6	9.64^7	2.85^4	0.84	5.94	0.320	0.054	3.98	1.12	0.281	3.98	14.82	3.73	0.64	$3.92^{-4}/2.62^{-4}$
B05	11.58	1.52^8	4.0^4	1.23	6.11	0 344	0.056	4.23	0.887	0.21	4.23	8.71	2.06	0.59	$3.46^{-4}/5.08^{-4}$

NOTE:

(1) All vehicles of sphere-cone type

(2) Nose material – ATJ graphite; frustum material – Beryllium (except B09 – which consists of a stainless steel nose and Inconel frustum)

(3) Numbers appearing as Z^b, should be read as $Z \times 10^b$

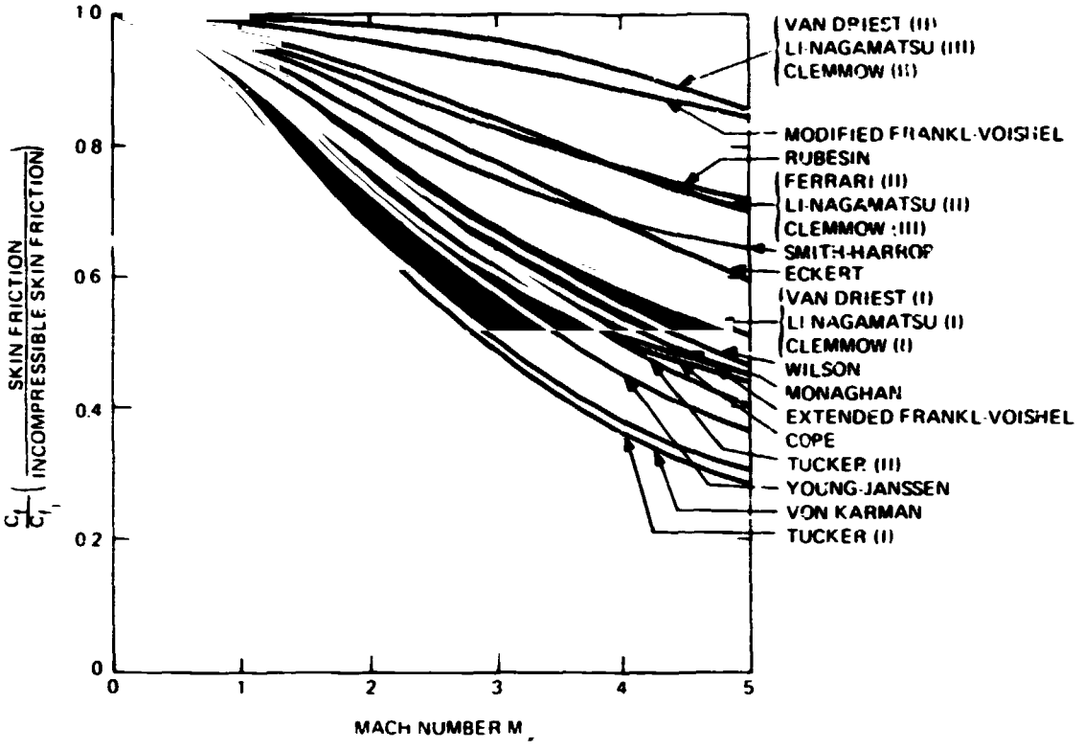

Figure 1. Comparison of Adiabatic Wall Turbulent Compressible Skin Friction Theories[2]

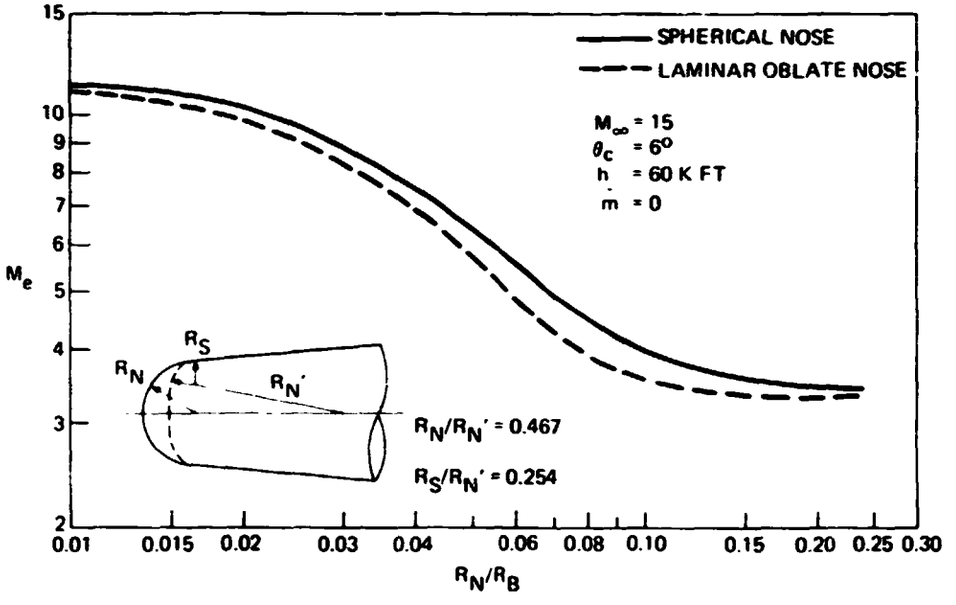

Figure 2. Effect of Nose Bluntness and Shape on the Local Mach Number at the End of the Vehicle (VIZAAD Result)

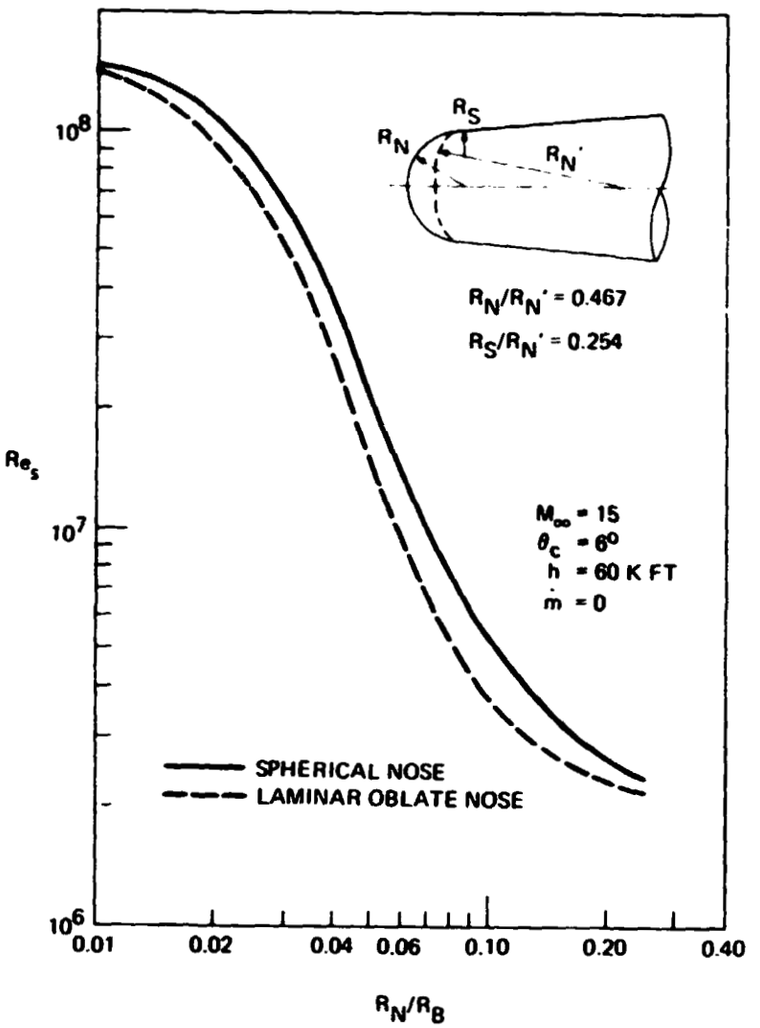

Figure 3. Effect of Nose Bluntness and Shape on the Local Reynolds Number at the End of the Vehicle (VIZAAD Result)

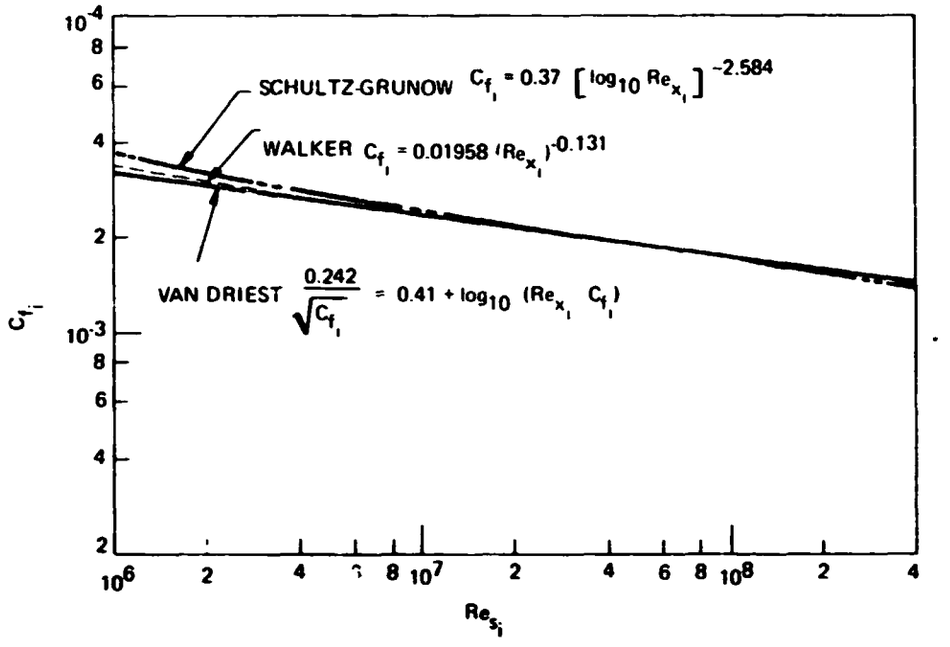
SCHULTZ-GRUNOW $C_{f_i} = 0.37 \left[\log_{10} Re_{x_i}\right]^{-2.584}$
WALKER $C_{f_i} = 0.01958 (Re_{x_i})^{-0.131}$
VAN DRIEST $\frac{0.242}{\sqrt{C_{f_i}}} = 0.41 + \log_{10} (Re_{x_i} C_{f_i})$
C_{f_i}
Re_{s_i}

Figure 4. Comparison of Skin-Friction Relationships with Wetted Length Reynolds Number

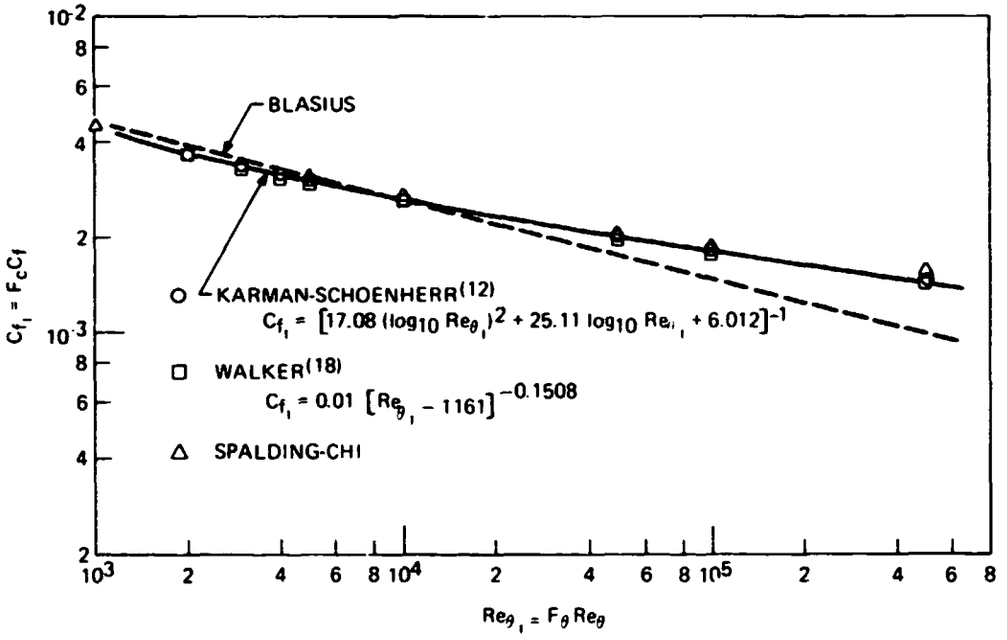

Figure 5. Comparison of Skin-Friction Relations with Momentum Thickness

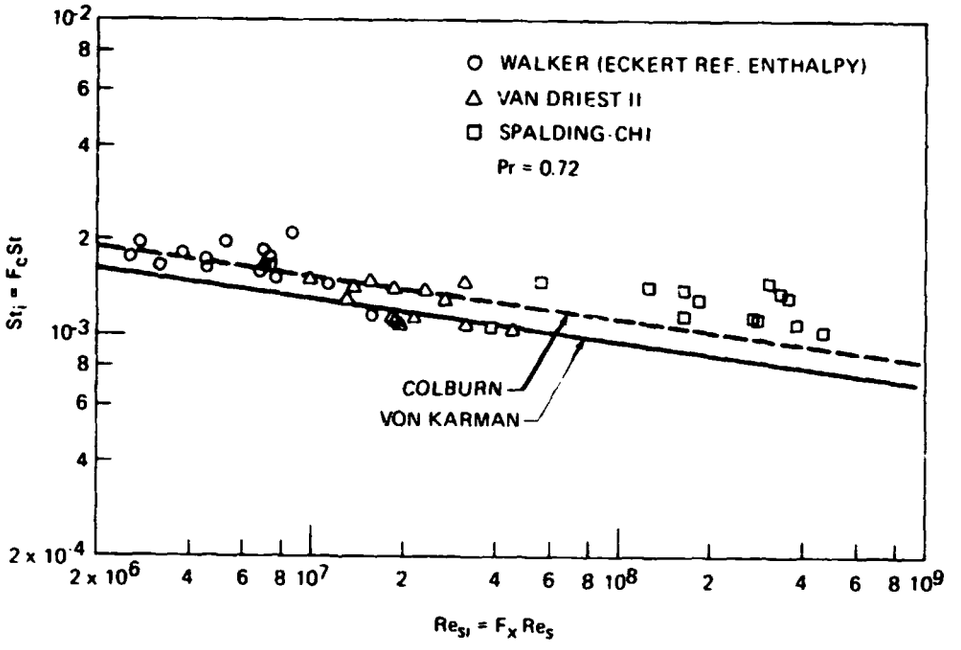

Figure 6. Transformed Turbulent Heating Data Based on Wetted Length

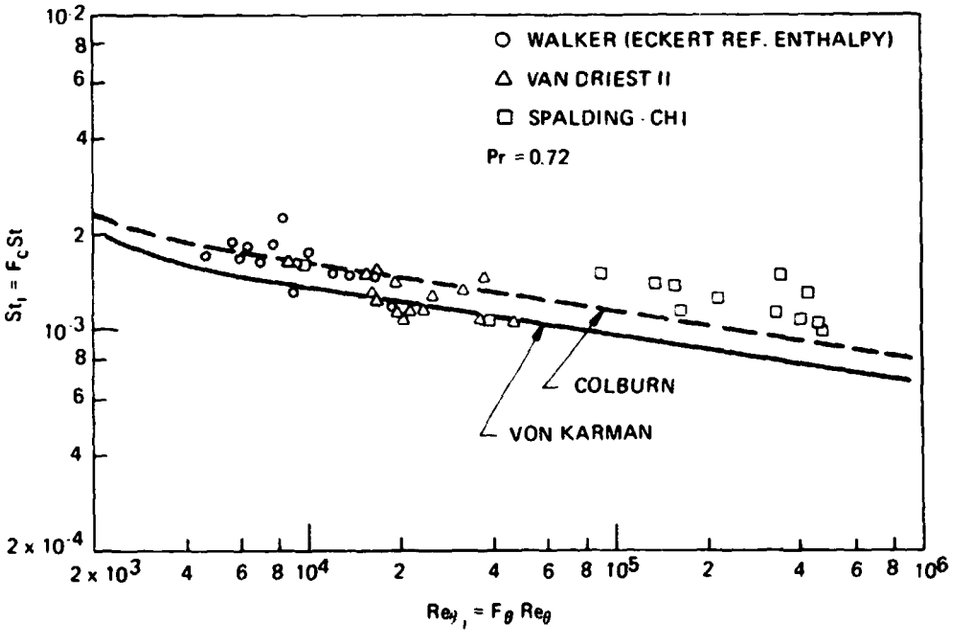

Figure 7. Transformed Turbulent Heating Data Based on Momentum Thickness